

Multiple dynamic transitions in nonequilibrium work fluctuations

Jae Dong Noh,^{1,2} Chulan Kwon,³ and Hyunggyu Park²

¹*Department of Physics, University of Seoul, Seoul 130-743, Korea*

²*School of Physics, Korea Institute for Advanced Study, Seoul 130-722, Korea*

³*Department of Physics, Myongji University, Yongin, Gyeonggi-Do, 449-728, Korea*

(Dated: February 23, 2012)

The time-dependent work probability distribution function $P(W)$ is investigated analytically for a diffusing particle trapped by an anisotropic harmonic potential and driven by a nonconservative drift force in two dimensions. We find that the exponential tail shape of $P(W)$ characterizing rare-event probabilities undergoes a sequence of dynamic transitions in time. These remarkable *locking-unlocking* type transitions result from an intricate interplay between a rotational mode induced by the nonconservative force and an anisotropic decaying mode due to the conservative attractive force. We expect that most of high-dimensional dynamical systems should exhibit similar multiple dynamic transitions.

PACS numbers: 05.70.Ln, 05.40.-a, 02.50.-r, 05.10.Gg

Systems in thermal equilibrium (EQ) are governed by the principle of statistical mechanics. It serves as the unified framework for the study of thermodynamic properties of EQ systems, and has been successful since it was established centuries ago. On the contrary, such a principle, except for the second law of thermodynamics, was absent for nonequilibrium (NEQ) systems, which made it difficult to understand NEQ phenomena. Recently, discovery of the fluctuation theorem (FT) opened a new perspective on NEQ processes and has attracted a lot of interests from researchers. The FT refers to identity relations for a thermodynamic quantity, such as work, heat, or entropy production, that are derived theoretically for a wide class of NEQ process [1–9], and are also confirmed experimentally [10–12]. It not only serves as a criterion diagnostic to NEQ, but also sheds light on quantitative understanding of NEQ fluctuations [13–17].

Consider a system which is in thermal EQ with a heat reservoir at the inverse temperature β . It is driven into a NEQ state by applying a nonconservative force [18] or making contact to other reservoirs at different temperatures [19–21]. The NEQ work W done on the system over a finite time interval is known to satisfy the integral FT, known as the Jarzynski equality (JE) $\langle e^{-\beta W} \rangle = 1$ [3, 8, 18]. The JE, being combined with the Jensen's inequality, yields $\langle W \rangle \geq 0$, which corresponds to the Kelvin statement of the thermodynamic second law. Furthermore, Crooks found that its probability distribution function (PDF) $P(W)$ satisfies the detailed FT such as $P(W)/P(-W) = e^{\beta W}$ [4]. It may deliver a surprising message that negative- W events are possible, however they are exponentially rare and thus one still finds the average work $\langle W \rangle \geq 0$.

The FT evokes the importance of studying NEQ fluctuations, especially in the rare-event region (e.g. negative W) to measure the violation of the thermodynamic second law in a small system. Many studies have been done for the PDF's of the work and heat associated with NEQ

processes, theoretically and experimentally [1–12, 18–20, 22, 23]. These are to confirm the FT in the first place, and then to investigate the nature of NEQ fluctuations. Normally it is a formidable task to find the PDF analytically for a specific NEQ process, so most studies are limited to special cases such as the large deviation study in the infinite-time limit [24–28].

In this Letter, we investigate the PDF of a NEQ work W over a *finite* time interval t in a two-dimensional linear diffusion system (LDS), driven by a nonconservative linear drift force. The LDS is often referred to as a multivariate Ornstein-Uhlenbeck process describing the motion of a Brownian particle or a particle trapped by a linear force in the overdamped limit [29, 30]. This system is simple enough that the PDF $P(W)$ is analytically tractable for finite time interval [18, 30] and still has many interesting experimental applications, e.g. a nano heat engine in contact with multiple heat reservoirs [19] and a colloidal particle driven along periodic potential imposed by laser traps [15]. Our study reveals that even such a simple system displays a surprisingly rich dynamic behavior with a sequence of dynamic transitions in time.

We briefly summarize the results with dimensionless W in units of $1/\beta$: (i) The PDF has exponential tails with power-law prefactors as $P(W) \sim |W|^{-\alpha_{\pm}} e^{-W/W_{\pm}}$ in the $W \rightarrow \pm\infty$ limit. The power-law exponents are the same in both sides ($\alpha_+ = \alpha_- = \alpha$), and the characteristic works $W_+ > 0$ and $W_- < 0$ satisfy $1/W_+ + 1/W_- = -1$, which are required for the detailed FT. (ii) The power-law exponent α can take three different values of 0, 1/2, and 2. Accordingly, the PDF is categorized into type 0 with $\alpha = 0$, type I with $\alpha = 1/2$, and type II with $\alpha = 2$. Interestingly, W_{\pm} continuously varies with time t for type 0 and type I, while they are constants of time for type II. (iii) Typically, the system undergoes a dynamic transition from type I to type II as t increases. The characteristic work W_+ increases smoothly with t and suddenly becomes frozen at the transition time t_c and afterwards.

This is a kind of a *locking* transition. More remarkably, in some parameter space, the PDF alternates between type I and type II indefinitely, i.e. infinite number of locking-unlocking type transitions. In general, a finite sequence of dynamic transitions is also possible as well as no transition with type I in all time. Type 0 is found without any dynamic transition, only in a special case.

We consider a LDS with the equations of motion

$$\frac{d\mathbf{q}}{dt} = -\mathbf{F} \cdot \mathbf{q} + \boldsymbol{\xi} \quad (1)$$

where $\mathbf{q} = (q_1, \dots, q_d)^T$ is a d -dimensional vector, $\mathbf{F} = (F_{ij})$ is a constant positive-definite ($d \times d$) force matrix, and $\boldsymbol{\xi}(t) = (\xi_1(t), \dots, \xi_d(t))^T$ is the Langevin noise satisfying

$$\langle \xi_i(t) \rangle = 0, \quad \langle \xi_i(t) \xi_j(t') \rangle = 2D_{ij} \delta(t - t') \quad (2)$$

with a noise correlation matrix $\mathbf{D} = (D_{ij})$ which is symmetric and positive-definite. After a similarity and a scale transformation, one can take the noise matrix as the identity matrix \mathbf{I} ($\mathbf{D} = \mathbf{I}$) without loss of generality.

One can decompose the force matrix into the conservative and nonconservative parts as $\mathbf{F} = \mathbf{F}_c + \mathbf{F}_{nc}$ with $\mathbf{F}_c = \mathbf{F}_c^T$. \mathbf{F}_{nc} is not symmetric to generate a nonconservative force. When $\mathbf{F}_{nc} = 0$, the total force $\mathbf{f} = -\mathbf{F} \cdot \mathbf{q}$ is conservative and can be represented as a minus gradient of a potential function $V(\mathbf{q}) = \frac{1}{2} \mathbf{q}^T \cdot \mathbf{F} \cdot \mathbf{q}$. The steady-state PDF is given by the EQ Boltzmann distribution $P_{eq}(\mathbf{q}) \propto e^{-V(\mathbf{q})}$ satisfying the detailed balance condition. A nonsymmetric force matrix ($\mathbf{F}_{nc} \neq 0$) indicates the presence of a nonconservative force $\mathbf{f}_{nc} = -\mathbf{F}_{nc} \cdot \mathbf{q}$ which cannot be written as a gradient function. It drives the system out of EQ. Here, we only consider the anti-symmetric \mathbf{F}_{nc} ($= -\mathbf{F}_{nc}^T$) for simplicity [31].

Suppose that the system is prepared in the thermal EQ with $P_{eq}(\mathbf{q}) \propto e^{-(1/2)\mathbf{q}^T \cdot \mathbf{F}_c \cdot \mathbf{q}}$ with the conservative force $\mathbf{f}_c = -\mathbf{F}_c \cdot \mathbf{q}$ only, then turn on the nonconservative force \mathbf{f}_{nc} at $t = 0$. The NEQ work (done by \mathbf{f}_{nc}) on the particle following a path $\mathbf{q}(\tau)$ for $0 \leq \tau \leq t$ is given by

$$\mathcal{W}[\mathbf{q}(\tau)] = - \int_0^t d\tau \frac{d\mathbf{q}(\tau)^T}{d\tau} \cdot \mathbf{F}_{nc} \cdot \mathbf{q}(\tau). \quad (3)$$

Defining the PDF $P(W) = \langle \delta(W - \mathcal{W}[\mathbf{q}(\tau)]) \rangle$ and its characteristic function $\mathcal{G}(t; \lambda) = \int dW e^{-\lambda W} P(W)$, we obtain [18]

$$\ln \mathcal{G}(t; \lambda) = - \int_0^t d\tau \text{Tr}(\tilde{\mathbf{A}}(\tau; \lambda) - \tilde{\mathbf{F}}) - \frac{1}{2} \ln \frac{\det \tilde{\mathbf{A}}(t; \lambda)}{\det \mathbf{F}_c}. \quad (4)$$

Here, the symmetric ($d \times d$) matrix $\tilde{\mathbf{A}}$ is the solution of

$$\frac{d}{d\tau} \tilde{\mathbf{A}}(\tau; \lambda) = -2\tilde{\mathbf{A}}^2 + \tilde{\mathbf{A}}\tilde{\mathbf{F}} + \tilde{\mathbf{F}}^T \tilde{\mathbf{A}} + \boldsymbol{\Lambda} \quad (5)$$

with the initial condition $\tilde{\mathbf{A}}(0) = \mathbf{F}_c$, and the auxiliary matrices are defined as $\tilde{\mathbf{F}}(\lambda) = \mathbf{F} - 2\lambda \mathbf{F}_{nc}$ and $\boldsymbol{\Lambda}(\lambda) = (\mathbf{F}^T \mathbf{F} - \tilde{\mathbf{F}}^T \tilde{\mathbf{F}})/2$ [18].

We apply the formalism to a two-dimensional system with the force matrices, parameterized as

$$\mathbf{F}_c = \begin{pmatrix} 1+u & v \\ v & 1-u \end{pmatrix}, \quad \mathbf{F}_{nc} = \begin{pmatrix} 0 & \varepsilon \\ -\varepsilon & 0 \end{pmatrix}, \quad (6)$$

with $u \geq 0$ and $\varepsilon \geq 0$. One can set the trace of \mathbf{F} to any positive number by the global rescaling of \mathbf{q} and t . Here, it is set to be 2. Positive-definiteness of \mathbf{F} and \mathbf{F}_c requires that $\sigma^2 \equiv u^2 + v^2 < 1$. The equations of motion are covariant under rotation, and ε and σ are invariant. So we may take $v = 0$ without loss of generality. Note that the parameter ε corresponds to the strength of NEQ driving (torque), while the parameter σ represents the anisotropy of the harmonic potential.

Before considering the general case, we present the solution in the special isotropic case with $u = v = 0$. In this case, the matrix $\tilde{\mathbf{A}}$ is proportional to the identity matrix \mathbf{I} as $\tilde{\mathbf{A}} = z(\tau; \lambda) \mathbf{I}$. Then, Eq. (5) becomes $dz/d\tau = -2z^2 + 2z + 2\varepsilon^2 \lambda(1 - \lambda)$ with $z(0) = 1$ and Eq. (4) is written as

$$\ln \mathcal{G}(t; \lambda) = -2 \int_0^t (z(\tau; \lambda) - 1) d\tau - \ln z(t; \lambda). \quad (7)$$

The solution of the differential equation is given by

$$z(\tau; \lambda) = \frac{1}{2} \left(1 + \frac{\sqrt{\Delta} (1 + \sqrt{\Delta} \tanh(\sqrt{\Delta} \tau))}{\sqrt{\Delta} + \tanh(\sqrt{\Delta} \tau)} \right) \quad (8)$$

where

$$\Delta \equiv 1 - 4\varepsilon^2 \lambda(\lambda - 1) > 0. \quad (9)$$

At $\Delta = 0$, we have $z(\tau; \lambda) = \frac{1}{2} + \frac{1}{2(\tau+1)}$. For negative Δ , the solution in Eq. (8) should be continued analytically using $\tanh(i\epsilon) = i \tan(\epsilon)$. Examining the above equations, we draw the following conclusions: (i) Since $\Delta(\lambda) = \Delta(1 - \lambda)$, one finds $\mathcal{G}(t; \lambda) = \mathcal{G}(t; 1 - \lambda)$ at all t . This verifies the Crooks detailed FT. (ii) Given t , there exists $\lambda_0(t) > 1$ such that $z(t; \lambda = \lambda_0) = z(t; \lambda = 1 - \lambda_0) = 0$. The logarithmic term in Eq. (7) tells us that the characteristic function has a divergence as $\mathcal{G}(t; \lambda) \sim (\lambda_0 - \lambda)^{-1}$ as $\lambda \rightarrow \lambda_0$ from below. There is the same divergence at $\lambda = 1 - \lambda_0$. (iii) The simple poles manifest the exponential tails of $P(W)$:

$$P(W) \sim \begin{cases} e^{-(\lambda_0(t)-1)W} & , W \rightarrow \infty \\ e^{-\lambda_0(t)|W|} & , W \rightarrow -\infty \end{cases} \quad (10)$$

where $\lambda_0(t)$ monotonically decreases in t and asymptotically approaches to $\lambda_c = \frac{1}{2} + \sqrt{1 + \varepsilon^2}/(2\varepsilon) \geq 1$. This PDF belongs to type 0. (iv) The large deviation function $e(\lambda) = -\lim_{t \rightarrow \infty} \frac{1}{t} \ln \mathcal{G}(t; \lambda)$ exists and is given by $e(\lambda) = \sqrt{\Delta(\lambda)} - 1$ for $\Delta(\lambda) \geq 0$ and $-\infty$, otherwise.

The analysis above gives us a lesson that the singularity of \mathcal{G} , hence the tail behavior of $P(W)$, is determined from the root of $\det \tilde{\mathbf{A}}(t; \lambda) = 0$. In the special

case ($u = v = 0$), two eigenvalues of $\tilde{\mathbf{A}}$ are degenerate. So, the root contributes to a simple pole of \mathcal{G} and the pure exponential tail of $P(W)$. When the degeneracy is broken, which is the case for any nonzero value of u or v , \mathcal{G} has a square-root singularity at the root and one may expect the PDF of type I. However, the actual behavior is much richer and can be understood from the full solution of Eq. (5).

Here, we sketch briefly the way to find the exact solution of Eq. (5). Details will be published elsewhere [32]. First, one needs to find a fixed-point solution $\tilde{\mathbf{A}}_s(\lambda)$ such that $\frac{d\tilde{\mathbf{A}}}{d\tau}\Big|_{\tilde{\mathbf{A}}=\tilde{\mathbf{A}}_s} = 0$. It can be expressed as

$$\tilde{\mathbf{A}}_s = \frac{1}{2}(\tilde{\mathbf{F}} + \mathbf{V}\mathbf{F}), \quad (11)$$

where an orthogonal matrix \mathbf{V} ($\mathbf{V}\mathbf{V}^T = \mathbf{I}$) is to satisfy $\mathbf{F}^T\mathbf{V}^T - \mathbf{V}\mathbf{F} = \tilde{\mathbf{F}} - \tilde{\mathbf{F}}^T$ to ensure $\tilde{\mathbf{A}}_s^T = \tilde{\mathbf{A}}_s$. Then, the matrix $\mathbf{R}(\tau; \lambda) = (\tilde{\mathbf{A}} - \tilde{\mathbf{A}}_s)^{-1}$ satisfies a linear differential equation

$$\frac{d\mathbf{R}}{d\tau} = 2\mathbf{I} - \mathbf{R}\hat{\mathbf{F}}^T - \hat{\mathbf{F}}\mathbf{R}, \quad (12)$$

where $\hat{\mathbf{F}}(\lambda) \equiv \tilde{\mathbf{F}} - 2\tilde{\mathbf{A}}_s$ and the initial condition is given by $\mathbf{R}(0) = (\tilde{\mathbf{A}}(0) - \tilde{\mathbf{A}}_s)^{-1}$. Its solution is

$$\begin{aligned} \mathbf{R}(\tau; \lambda) &= e^{-\tau\hat{\mathbf{F}}} \mathbf{R}(0; \lambda) e^{-\tau\hat{\mathbf{F}}^T} + 2 \int_0^\tau d\tau' e^{-\tau'\hat{\mathbf{F}}} e^{-\tau'\hat{\mathbf{F}}^T} \\ &= \mathbf{R}_\infty + e^{-\tau\hat{\mathbf{F}}} (\mathbf{R}(0; \lambda) - \mathbf{R}_\infty) e^{-\tau\hat{\mathbf{F}}^T}, \end{aligned} \quad (13)$$

where $\mathbf{R}_\infty \equiv \hat{\mathbf{F}}^{-1}(\mathbf{I} + \hat{\mathbf{Q}})$ with the antisymmetric matrix $\hat{\mathbf{Q}}$ satisfying $\hat{\mathbf{F}}\hat{\mathbf{Q}} + \hat{\mathbf{Q}}\hat{\mathbf{F}}^T = \hat{\mathbf{F}} - \hat{\mathbf{F}}^T$ [18]. Finally, one obtains the full time-dependent solution

$$\tilde{\mathbf{A}}(\tau; \lambda) = \tilde{\mathbf{A}}_s + \mathbf{R}(\tau; \lambda)^{-1} \quad (14)$$

of Eq. (5) in any d dimension. Associated algebra is rather simple in two dimensions. We find $\hat{\mathbf{Q}} = (\hat{\mathbf{F}} - \hat{\mathbf{F}}^T)/\text{Tr}\hat{\mathbf{F}}$ and \mathbf{V} is also easily determined. The explicit expression for Eq. (14) is still rather complex, which will appear in [32].

The solution is just the starting point for further analysis of the PDF. We found that $\det \tilde{\mathbf{A}}(t; \lambda)$ exhibits a complex behavior depending on the parameter values of ε , u , and v . There are four distinct cases, which are shown in Fig. 1. The plots are obtained for a few values of u to a given $\varepsilon = 3/10$. We took $v = 0$ since only $\sigma = \sqrt{u^2 + v^2}$ is the relevant parameter.

(i) When u is small enough (see Fig. 1(a)), the curve is not tangential to the τ axis at any value of λ . For any given $\tau = t$, one can find λ_0 such that $\det \tilde{\mathbf{A}}(\tau, \lambda_0) = 0$ (non-degenerate root). Then, $\det \tilde{\mathbf{A}}(t, \lambda) \sim (\lambda_0 - \lambda)$ near $\lambda \simeq \lambda_0$ and, from Eq. (4), $\mathcal{G}(t, \lambda) \sim (\lambda_0 - \lambda)^{-1/2}$. Hence, the PDF has a tail $P(W) \sim |W|^{-1/2} e^{\lambda_0 W}$ in the $W \rightarrow -\infty$ limit (type I), with $\lambda_0 = \lambda_0(t)$ monotonically decreasing with t to an asymptotic value $\lambda_c(u, \varepsilon) > 1$.

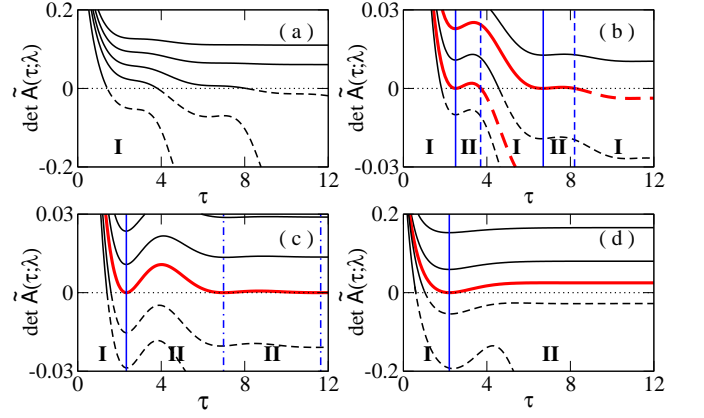


FIG. 1. (Color online) Time evolution of $\det \tilde{\mathbf{A}}(\tau; \lambda)$ when $\varepsilon = 3/10$ and (a) $u = 0.65$, (b) 0.7 , (c) $u^* = \sqrt{109/200}$, and (d) 0.8 with several values of $\lambda > 1$ (lower curves represent larger values of λ). The curves tangential to the τ axis (dotted horizontal line) are drawn with thick lines (red). The characteristic function \mathcal{G} is well defined only when $\det \tilde{\mathbf{A}} > 0$. Curves in the unphysical regions with $\det \tilde{\mathbf{A}} < 0$ are plotted with dashed lines.

(ii) In the intermediate values of u (see Fig. 1(b)), the curve is tangential to the τ axis at multiple values of λ . We will denote the time for the n -th tangential point as t_n^+ (marked with vertical solid lines) and the corresponding λ value as λ_n . The curve, $\det \tilde{\mathbf{A}}(\tau, \lambda_n)$, that is tangential at $\tau = t_n^+$ may cross the τ axis at a later time denoted as $\tau = t_n^-$ (marked with vertical dashed lines). This crossing is linear (non-degenerate root) and never happens again later. Within the time interval $t_n^+ < t < t_n^-$, the characteristic function $\mathcal{G}(t; \lambda)$ is finite for $\lambda < \lambda_n$, and then it diverges discontinuously at $\lambda = \lambda_n$. Hence the PDF has a tail $P(W) \sim |W|^{-2} e^{\lambda_n W}$ in the $W \rightarrow -\infty$ limit (type II) [33]. Note that λ_n is a constant of time within the finite time interval. Outside the interval, the PDF belongs to type I. Hence, the PDF alternates between type I and type II many times as t increases.

(iii) At the special value of $u = u^* \equiv \sqrt{(1 + \varepsilon^2)/2}$, the curve, $\det \tilde{\mathbf{A}}(\tau, \lambda^*)$, with $\lambda^* = (1 + \varepsilon)/(2\varepsilon)$ is tangential to the τ axis infinitely many times as

$$\det \tilde{\mathbf{A}}(\tau; \lambda^*) = \frac{\varepsilon(1 - \varepsilon)(1 + \varepsilon)(1 + \cos \omega \tau)}{4 \left(e^{2\varepsilon \tau} - \frac{1 - \varepsilon}{1 + \varepsilon} - \varepsilon \frac{1 - \varepsilon}{1 + \varepsilon} \cos \omega \tau \right)}, \quad (15)$$

with $\omega = \sqrt{2(1 - \varepsilon^2)}$ and the tangential points at $t_n^+ = (2n - 1)\pi/\omega$ ($n = 1, 2, \dots$). Note that $t_n^- = t_{n+1}^+$. Hence, the PDF belongs to type I when $t < t_1^+$ (marked with the vertical solid line) and changes to type II afterwards except periodic instantaneous moments at $t = t_n^+$ ($n \geq 2$) (marked with vertical dot-dashed lines).

(iv) When $u > u^*$, the curve is tangential to the τ axis at a single value of λ at $\tau = t_1^+$ (marked with the vertical solid line) without crossing the τ axis later. Hence, the PDF belongs to type I for $\tau < t_1^+$ and type II afterwards

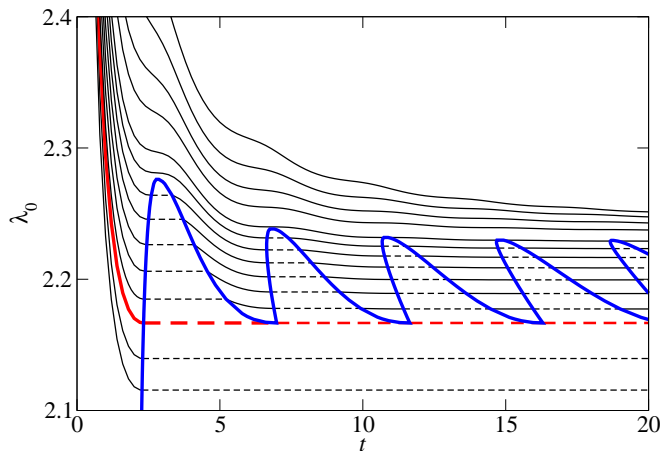


FIG. 2. (Color online) Constant- x curves in the λ_0 - t plane at $\varepsilon = 3/10$. The value of u ranges from 0.55 (top) to 0.76 (bottom). The solid curves correspond to the PDF of type I, while the dashed line corresponds to the PDF of type II with the boundary drawn with the thick zigzag (blue) curve. The thick (red) curve corresponds to the case with $u = u^*$.

forever.

Our analysis reveals that the system undergoes a dynamic transition in the tail shape of the PDF between type I characterized by $P(W) \sim |W|^{-1/2} e^{\lambda_0 W}$ and the type II characterized by $P(W) \sim |W|^{-2} e^{\lambda_0 W}$ for large negative W . The same applies for large positive W due to the symmetry of the detailed FT, see Eq. (10). The parameter λ_0 , which corresponds to the inverse of the characteristic fluctuation size $|W_-|$ for the negative PDF tail, decreases continuously in time for type I, while it is locked for type II. For example, in case of (ii), λ_0 decreases up to $t = t_1^+$, and is locked for a while till $t = t_1^-$, then is unlocked at $t = t_2^+$ and decreases again till $t = t_2^-$, and so on. These locking-unlocking transitions occur many times as t goes by.

The transition moments can be found numerically exactly from the roots of $\det \hat{A}(\tau; \lambda) = 0$, using the solution given in Eq. (14). We present the constant- u curves in the λ_0 - t plane at $\varepsilon = 3/10$ in Fig. 2. The PDF undergoes a single dynamic transition for large values of u , infinitely many transitions for intermediate values of u , and no transition for small u . From the constant- u curves, one can construct the phase diagram in the u - t plane. The phase diagram is drawn in Fig. 3.

In summary, our analytic result shows that such a simple linear diffusion system exhibits surprisingly complex NEQ fluctuations. It raises interesting questions for the mechanism of the dynamic transition. The conservative part of the drift force generates an anisotropic harmonic potential, which attracts the particle toward the origin. The nonconservative part acts like a torque, which drives the particle into a rotational motion. It is useful to introduce the polar coordinate to focus on the rotational dynamics separately. Then, the dynamics of the polar angle

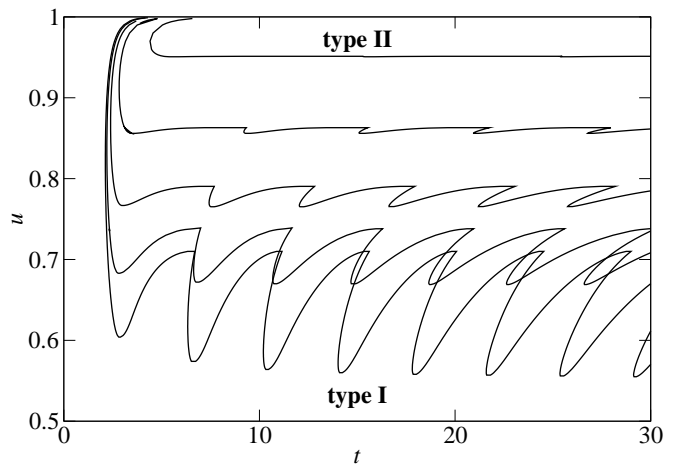


FIG. 3. Phase diagram in the u - t plane for several values of $\varepsilon = 0.1$ (bottom), 0.3, 0.5, 0.7, and 0.9 (top). The PDF belongs to type II in the region surrounded by the phase boundary curve, and type I elsewhere except the line $u = 0$ where the type-0 PDF is found. For $\varepsilon \geq 1$, the phase boundary disappears completely and no type II exists.

may be written down effectively as $d\phi/dt = a \sin \phi + b + \xi$, where the potential amplitude a should be proportional to the anisotropy σ and the constant driving force b should be proportional to the strength of the nonconservative force ε . This is the equation of motion in a tilted periodic potential [15]. For $a \ll b$ (small σ), the particle has no time to relax in the potential well and drifts down into the steady state with a constant velocity. So there is no extra time scale except for the relaxation into the steady state. Thus, we expect no dynamic transitions and type-I PDF forever. For $a \gg b$ (large σ), the particle sits at the potential well long enough and fully relaxes inside the well. Then, it can hop to the neighboring well due to the noise after a finite time, which can be determined by the noise strength. This additional time scale exists and may set the transition time t_1^+ . As the particle relaxation in the first well is fully developed already, there will be no additional time scale needed for successive hoppings. Thus, we expect one dynamic transition from type-I to type-II PDF. When $a \approx b$ (intermediate σ), it needs additional time scales for successive hoppings with incomplete relaxations within each potential well, which leads to multiple dynamic transitions. The above argument provides a plausible understanding of existence of multiple time scales, but does not fully capture underlying mechanisms of dynamic locking-unlocking transitions. Since the radial component also fluctuates in our model, there are more possible complex routes to relax into the steady state. It is remarkable to find no smearing out of sharp dynamic transitions with fully locking states. We leave full intuitive physical understanding of these dynamic transitions for future works.

As can be seen in our analysis, the remarkable char-

acteristics of multiple dynamic transitions should not be a pathological property of some special systems. Hence, we expect that any high-dimensional dynamical system driven by a nonconservative force should exhibit similar or more complex multiple dynamic transitions in a reasonably large parameter space. It would be interesting to observe these locking-unlocking features in experimental setups such as in [15, 19] by measurements in transient regime.

H.P. thanks David Mukamel and Haye Hinrichsen for useful discussions. This work was supported by the Mid-career Researcher Program through the NRF Grant No. 2010-0026627 and also by the NRF grant No. 2012-0005003 (JDN) funded by MEST.

-
- [1] D. J. Evans, E. G. D. Cohen, and G. P. Morriss, Phys. Rev. Lett. **71**, 2401 (1993).
- [2] G. Gallavotti and E. G. D. Cohen, Phys. Rev. Lett. **74**, 2694 (1995).
- [3] C. Jarzynski, Phys. Rev. Lett. **78**, 2690 (1997).
- [4] G. E. Crooks, Phys. Rev. E **60**, 2721 (1999).
- [5] J. Lebowitz and H. Spohn, J. Stat. Phys. **95**, 333 (1999).
- [6] T. Hatano and S.-I. Sasa, Phys. Rev. Lett. **86**, 3463 (2001).
- [7] U. Seifert, Phys. Rev. Lett. **95**, 040602 (2005).
- [8] J. Kurchan, J. Stat. Mech.: Theor. Exp. 2007, P07005 (2007).
- [9] J. D. Noh and J.-M. Park, Phys. Rev. Lett. **108**, 240603 (2012).
- [10] D. Collin, F. Ritort, C. Jarzynski, S. B. Smith, I. Tinoco, and C. Bustamante, Nature **437**, 231 (2005).
- [11] N. Garnier and S. Ciliberto, Phys. Rev. E **71**, 060101 (2005).
- [12] S. Ciliberto, S. Joubaud, and A. Petrosyan, J. Stat. Mech. P12003 (2010).
- [13] T. Harada and S.-I. Sasa, Phys. Rev. Lett. **95**, 130602 (2005).
- [14] T. Speck and U. Seifert, Europhys. Lett. **74**, 391 (2006).
- [15] V. Blickle, T. Speck, C. Lutz, U. Seifert, and C. Bechinger, Phys. Rev. Lett. **98**, 210601 (2007); T. Speck, V. Blickle, C. Bechinger, and U. Seifert, EPL **79**, 30002 (2007).
- [16] J. Prost, J.-F. Joanny, and J. M. R. Parrondo, Phys. Rev. Lett. **103**, 090601 (2009).
- [17] K. Mallick, M. Moshe, and H. Orland, J. Phys. A **44**, 095002 (2011).
- [18] C. Kwon, J. D. Noh, and H. Park, Phys. Rev. E **83**, 061145 (2011).
- [19] R. Filliger and P. Reimann, Phys. Rev. Lett. **99**, 230602 (2007).
- [20] J.S. Lee, C. Kwon, and H. Park, arXiv:1209.5815.
- [21] For simplicity, we exclude a time-dependent perturbation, here.
- [22] R. van Zon and E. G. D. Cohen, Phys. Rev. Lett. **91**, 110601 (2003); Phys. Rev. E **69**, 056121 (2004).
- [23] R. van Zon, S. Ciliberto, and E. G. D. Cohen, Phys. Rev. Lett. **92**, 130601 (2004); S. Ciliberto, S. Joubaud, and A. Petrosyan, J. Stat. Mech. P12003 (2010).
- [24] J. Farago, J. Stat. Phys. **107**, 781 (2002).
- [25] H. C. Fogedby and A. Imparato, J. Stat. Mech. (2011) P05015.
- [26] P. Visco, J. Stat. Mech. (2006) P06006.
- [27] J. B. Weiss, Phys. Rev. E **76**, 061128 (2007).
- [28] A. Puglisi, L. Rondoni, and A. Vulpiani, J. Stat. Mech. (2006) P08010.
- [29] C.W. Gardiner, *Stochastic Methods: A Handbook for the Natural and Social Sciences* (Springer, Berlin, 2009).
- [30] H. Risken, *The Fokker-Planck Equation: Methods of Solution and Applications* (Springer, New York, 1989).
- [31] A nonconservative force matrix needs not be antisymmetric, in general (see [18]).
- [32] J. D. Noh, C. Kwon, H. Park, unpublished.
- [33] Detailed analysis of Type II can be found in [18].